Lz-Transform Approach for Fault Tolerance Assessment of Various Traction Drives Topologies of Hybrid-Electric Helicopter

Ilia Frenkel, Igor Bolvashenkov, Hans-Georg Herzog and Lev Khvatskin

Abstract This chapter presents a preliminary analysis of fault tolerance, availability and performance assessment of the two promising options of the hybrid-electric traction drive version for the helicopter, which can be treated as multi-state system, where components and entire system in general case have an arbitrary finite number of states corresponding to the different performance rates. The performance rate (output nominal power) of the system at any time instant is interpreted as a discrete-state continuous-time stochastic process. In the present chapter, the *Lz*-transform is applied to a real multi-state hybrid-electric traction drive version for the helicopter system that is functioning under various stochastic demands and its availability and performance is analyzed. It is shown that *Lz*-transform application drastically simplifies the availability computation for such a system compared with the straightforward Markov method.

Keywords Hybrid-electric traction drive · Availability · Performance assessment · *Lz*-transform · Multi-state system · Discrete-state continuous-time stochastic process

1 Introduction

Nowadays, the electrification of aircraft of different types and purposes is one of the most promising directions in the development of aviation technology. According to program MEA (More Electric Aircraft) [7] developers of various specialized companies are planning the creation of electric airplanes (liner, regional, special

I. Frenkel (✉) · L. Khvatskin
Center for Reliability and Risk Management, Sami Shamoon College of Engineering, Beer Sheva, Israel
e-mail: iliaf@sce.ac.il

I. Bolvashenkov · H.-G. Herzog
Institute of Energy Conversion Technology, Technical University of Munich, Munich, Germany

A. Lisnianski et al. (eds.), *Recent Advances in Multi-state Systems Reliability*, Springer Series in Reliability Engineering, DOI 10.1007/978-3-319-63423-4_17

purpose, manned and unmanned) as well as the helicopters (from heavy to small-size, manned and unmanned), which have a number of benefits associated with the improvement of the technical performance of the aircraft, increase their environmental performance and reducing operating costs.

The construction of electric aircraft requires a comprehensive revision of the principles of construction of a variety of devices and systems of the aircraft, which is associated with the creation of the new, having a low specific weight controlled electric drive, electric power generators, electrical energy storage (batteries, fuel cells, ultra-capacitors etc.), and electric power converters. The most important place in the solving the problem of the creation of electric aircrafts takes traction electric drive. The use of electrical technologies could lead in the near future to the changing the principles of its construction and propulsion.

The first step in the aircraft electrification is the development and implementation of hybrid-electric aircraft. This is due to the fact that today there are no electrical energy storages with high energy density and low weight and dimensions. Electric aircraft version can be implemented only with creation of new energy storage devices with the appropriate characteristics of the energy density, weight and dimensions.

This chapter presents a preliminary analysis of fault tolerance, availability and performance assessment of the two promising options of the hybrid-electric traction drive version for the conventional Airbus helicopter EC135/H135 with gas turbine engine and speed reducer [14].

Due to the system's nature, a fault in a single unit has only partial effect on the entire performance: it only reduces the system's performance. One partial failure of the traction multiphase permanent magnets synchronous motor leads to partial system failure (reduction of output nominal power), as well as the multiple consecutive multiphase motor's failures, to complete system failures. So, the hybrid-electric traction drive system can be treated as multi-state system (MSS), where components and entire system in the general case have an arbitrary finite number of states corresponding to different performance rates [1, 12, 13]. The performance rate (output nominal power) of the system at any time instant is interpreted as a discrete-state continuous-time stochastic process. Such a model is complex enough—even in relatively simple cases it has hundreds states. So, it is rather difficult to build the model and to solve the corresponding system of differential equations by using straightforward Markov method.

In recent years a specific approach called *Lz*-transform, was introduced [10] for discrete-state continuous-time Markov processes. This approach is an extension of the universal generating function (UGF) technique that was introduced by Ushakov [18] and has been widely applied to MSS reliability analysis [12]. *Lz*-transform was successfully applied to availability analysis of real-world multi-state systems under constant and variable demand [5, 6, 8, 11, 16] and its efficiency was demonstrated. In practice there are aging multi-state systems that are functioning under variable stochastic demand. In the present chapter, the *Lz*-transform is applied to a real MSS hybrid-electric traction drive version for the conventional helicopter system that is functioning under variable stochastic demand and its availability and performance is analyzed. It is shown that *Lz*-transform application drastically simplifies the availability computation for such a system compared with the straightforward Markov method.

2 Comparative Analysis of Two Traction Drive Topologies of Hybrid-Electric Helicopter

2.1 Common Description

In this chapter for the comparative analysis were selected two traction drive topologies of hybrid-electric helicopter: a serial electric-hybrid propulsion system with a gas turbine and electrical generator (Fig. 1a) and a combined electric-hybrid propulsion system with a gas turbine, generator and the speed reducer (Fig. 1b).

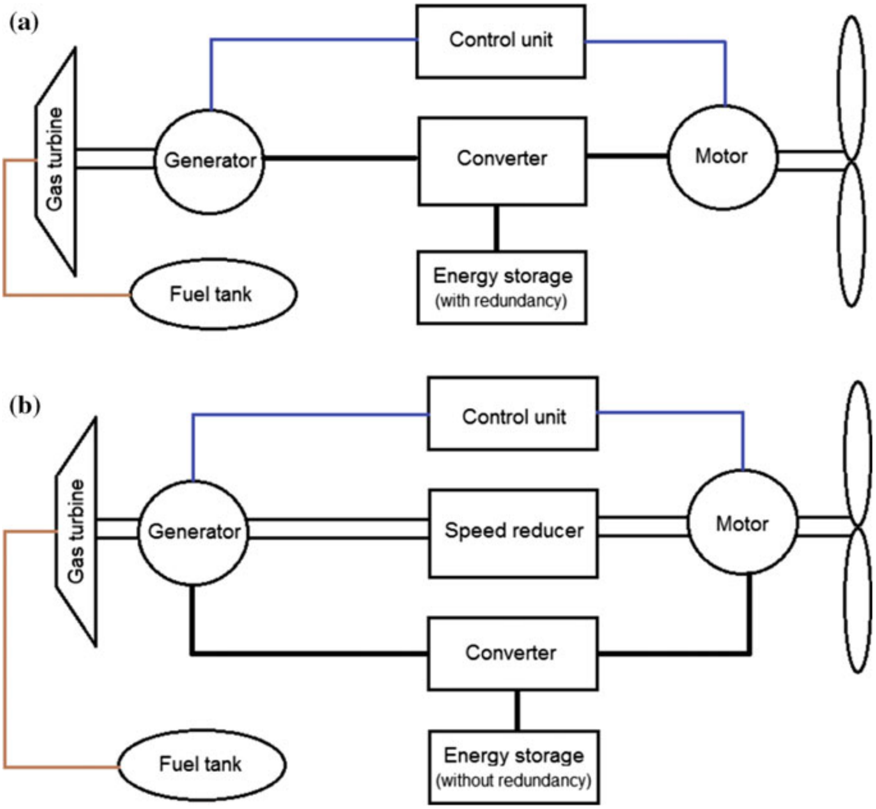

Fig. 1 Propulsion system topologies of the hybrid-electric helicopter, serial (**a**) and combined (**b**)

In these schemes the following equipment is used as follows:

- the GTE Pratt & Whitney of type PW206B2 [15] is used as the gas turbine engine,
- synchronous generator with permanent magnets [9] is used as an electric generator,
- the multiphase permanent magnets synchronous motor [4]—as the traction motor,
- multilevel cascaded H-bridge (CHB) inverter [3] is used as a converter and
- battery electric energy storage (BEES), based on the lithium-ion battery cells [2] —as energy storage.

As shown in [4], the optimal traction electric motor from the point of view of the helicopter's fault tolerance requirements is a 9-phase synchronous motor with permanent magnets and galvanically isolated phases. The states of degradation and the corresponding performance of the multiphase electric motors with the nominal power of 540 kW, which occur during the consecutive critical phase failures, is as follows: one phase failure reduces power to 480 kW, failure of two phases—to 420 kW, three phases' failure—to 360 kW. In this work, the power reduction less than 420 kW means full failure of the traction motor.

As shown in [3], the 17-level cascaded H-bridge inverter is the optimal type of electric converter in terms of helicopter's fault tolerance requirements.

The required power (demand) that must be implemented by the traction drive system of hybrid-electric helicopter for a one helicopter's flight is as follows: 540, 460 and 360 kW.

2.2 *Operational Scenarios for Various Traction Drive Topologies*

2.2.1 Serial Topology

In case of the serial topology (Fig. 1a) in normal failure-free operation, the gas turbine electric generator feeds the traction multiphase electric motor through the multilevel converter. The control unit controls the entire traction drive. The state of charge of battery cells is continually monitored, recharged from the electric generator and maintained at optimal maximum level. It is possible to install an additional amount of electric battery cells, which increase the fault tolerance indices of the battery electric energy storage of serial connection topology of traction drive units.

In failure case of the gas turbine engine or/and electric generator, depending on the value of electric energy storage capacity, it is possible, either the continuation of the flight to complete task performance, or a flight to a safe landing place. After landing the running repairs or complete replacement of the failed units are implemented.

2.2.2 Combined Topology

In case of the combined topology (Fig. 1b) in the normal failure-free operation there are two possible embodiment of the flight. In the first "electric" version of flight, the gas turbine electric generator feeds the multi-phase electric traction motor through multilevel inverter. In the second, the "mechanical" version of flight, the gas turbine engine directly rotates the propeller of the helicopter through a mechanical transmission and speed reducer. Control the components of the traction drive is carried out by the control unit. Electric battery storage is charged by the electrical generator only in the "electric" flight mode of helicopter.

In the failure case of electric generator, or/and an electric inverter, or/and the traction electric motor, the further flight is provided by "mechanical" embodiment of the traction drive scheme realization.

In the failure case of the speed reducer, the further flight is provided by "electrical" embodiment of the traction drive scheme realization.

In failure case of the gas turbine engine, a further short time flight to the safe landing of helicopter is carried out by electric energy of battery storage. After landing the running repairs or complete replacement of the failed units are implemented.

3 Brief Description of the *Lz*-Transform Method

We consider a multi-state system consisting of n multi-state components. Any j-component can have k_j different states, corresponding to different performances g_{ji}, represented by the set $\mathbf{g}_j = \{g_{j1}, \ldots, g_{jk_j}\}$, $j = \{1, \ldots, n\}$; $i = \{1, 2, \ldots, k_j\}$. The performance stochastic processes $G_j(t) \in \mathbf{g}_j$ and the system structure function $G(t) = f(G_1(t), \ldots, G_n(t))$ that produces the stochastic process corresponding to the output performance of the entire MSS, fully define the MSS model.

The MSS model definitions can be divided into the following steps. For each multi-state component we will build a model of stochastic process. Markov performance stochastic process for each component j can be represented by the expression $G_j(t) = \{\mathbf{g}_j, \mathbf{A}_j, \mathbf{p}_{j0}\}$, where $\mathbf{g}_j$ is the set of possible component's states, defined above, $\mathbf{A}_j = \left(a_{lm}^{(j)}(t)\right)$, $l, m = 1, \ldots, k; j = 1, \ldots n$ is the transition intensities matrix and $\mathbf{p}_{j0} = \left[p_{10}^{(j)} = \Pr\{G_j(0) = g_{10}\}, \ldots, p_{k_j0}^{(j)} = \Pr\{G_j(0) = g_{k_j0}\}\right]$ is the initial states probability distribution.

For each component j the system of Kolmogorov forward differential equations [17] can be written for determination of the state probabilities $p_{ji}(t) = \Pr\{G_j(t) = g_{ji}\}$, $i = 1, \ldots k_j, j = 1, \ldots, n$ under initial conditions $\mathbf{p}_{j0}$. Now *Lz*-transform of a discrete-state continuous-time (DSCT) Markov process $G_j(t)$ for each component j can be written as follows:

$$L_Z\left\{G_j(t)\right\} = \sum_{i=1}^{k_j} p_{ji}(t) z^{g_{ji}} \tag{1}$$

The next step, in order to find the *Lz*-transform of the entire MSS's output performance Markov process $G(t)$, the Ushakov's Universal Generating Operator [18] can be applied to all individual *Lz*-transforms $L_Z\left\{G_j(t)\right\}$ over all time points $t \geq 0$.

$$L_Z\{G(t)\} = \Omega_f\{L_Z[G_1(t)], \ldots, L_Z[G_n(t)]\} = \sum_{i=1}^{K} p_i(t) z^{g_i} \tag{2}$$

In this expression K is the number of states in the entire MSS, p_i and g_i are probabilities and performances of the entire MSS.

The technique of Ushakov's operator application is well established for many different structure functions [12].

Using the resulting *Lz*-transform MSS mean instantaneous availability for constant demand level w can be derived as sum all probabilities in *Lz*-transform from terms where powers of z are not negative:

$$A(t) = \sum_{g_i \geq w} p_i(t) \tag{3}$$

MSS's mean instantaneous performance may be calculated as sum all probabilities multiplied to performance in *Lz*-transform from terms where powers of z are positive:

$$E(t) = \sum_{g_i > 0} p_i(t) g_i \tag{4}$$

4 Multi-state Modeling of the Multi Power Source Traction Drive

4.1 Systems' Description

According to *Lz*-transform method, we build the Reliability Bloc Diagrams for presented on the Fig. 1 propulsion system topologies of the hybrid-electric helicopter. On Fig. 2 one can find the Reliability Block Diagram of the Serial Topology System and on Fig. 3—Reliability Block Diagram for Combined Topology System.

The main part of the Serial Topology System (STS) (Fig. 2) consists of two subsystems SS_{1s} and SS_{2s} connected in series. Subsystem SS_{1s} consists of 3 elements, Fuel Tank, Gas Turbine and Generator, connected in series. Subsystem SS_{2s} consists of 3 elements, Converter, Motor and Control Unit, connected in series. In

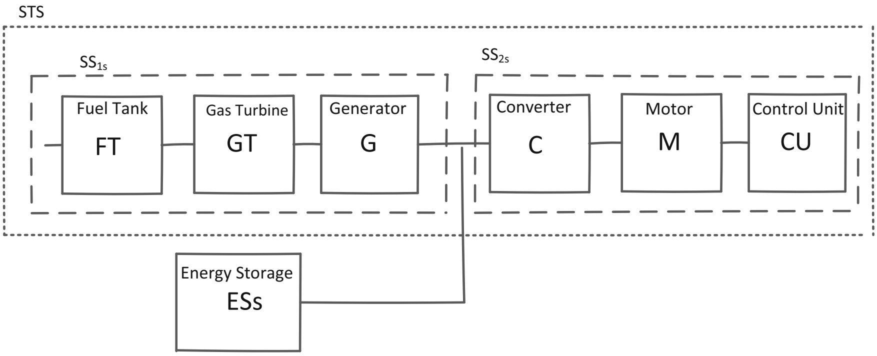

Fig. 2 Reliability Block Diagram of the Serial Topology System

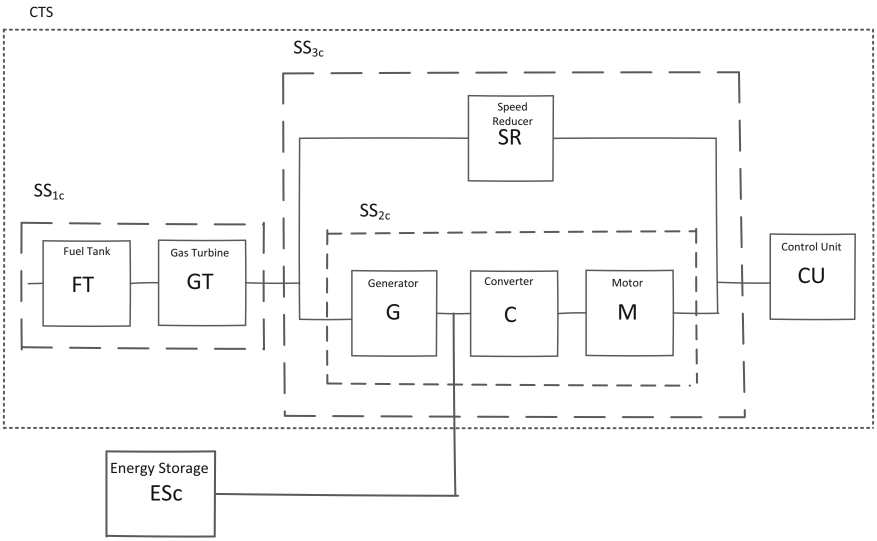

Fig. 3 Reliability Block Diagram of the Combined Topology System

case of emergency, instead main STS activates reserved system STS-ESs, where failed subsystem SS_{1s} replaced by multi-state Energy storage.

The main part of the Combined Topology System (CTS) (Fig. 3) consists of two subsystems SS_{1c} and SS_{3c} and Control Unit, connected in series. Subsystem SS_{1c} consists of 2 elements, Fuel Tank and Gas Turbine, connected in series. Subsystem SS_{3c} consists of Subsystem SS_{2c} and Speed Reducer, connected in parallel. Subsystem SS_{2c} consists of 3 elements, Generator, Converter and Motor, connected in series. In case of emergency, instead main CTS activates reserved system CTS-ESs, consists of connected in series Energy storage, Converter, Motor and Control Unit.

Elements' descriptions are presented in the next section.

4.2 Elements' Description

4.2.1 Elements with 2 States

For system's elements, which have 2 states (fully working and fully failed) in order to calculate probabilities of each state we build the state space diagram (Fig. 4) and the following system of differential equations:

$$\begin{cases} \frac{dp_{i1}(t)}{dt} = -\lambda_i p_{i1}(t) + \mu_i p_{i2}(t), \\ \frac{dp_{i2}(t)}{dt} = \lambda_i p_{i1}(t) - \mu_i p_{i2}(t). \end{cases}, i = \text{FT, GT, G, ESc, C, SR, CU}$$

Initial conditions are: $p_{i1}(0); p_{i2}(0) = 0.$

We used MATLAB® for numerical solution of these systems of DE to obtain probabilities $p_{i1}(t), p_{i2}(t)$ (i = FT, GT, G, ESc, C, SR, CU). Therefore, for such system's element the output performance stochastic processes can be obtained as follows:

$$\begin{cases} \mathbf{g}_i = \{g_{i1}, g_{i1}\} = \{540, 0\}, \\ \mathbf{p}_i(t) = \{p_{i1}(t), p_{i1}(t)\} \end{cases}.$$

Sets $\mathbf{g}_i, \mathbf{p}_i(t)$ i = FT, GT, G, ESC, C, SR, CU define Lz-transforms for each element as follows:

Fuel Tank: $L_z\{g^{FT}(t)\} = p_1^{FT}(t)z^{g_1^{FT}} + p_2^{FT}(t)z^{g_2^{FT}} = p_1^{FT}(t)z^{540} + p_2^{FT}(t)z^0.$

Gas Turbine: $L_z\{g^{GT}(t)\} = p_1^{GT}(t)z^{g_1^{GT}} + p_2^{GT}(t)z^{g_2^{GT}} = p_1^{GT}(t)z^{540} + p_2^{GT}(t)z^0.$

Generator: $L_z\{g^{G}(t)\} = p_1^{G}(t)z^{g_1^{G}} + p_2^{G}(t)z^{g_2^{G}} = p_1^{G}(t)z^{540} + p_2^{G}(t)z^0.$

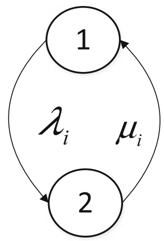

Fig. 4 State space diagram

Energy Storage

Combine: $L_z\{g^{ESc}(t)\} = p_1^{ESc}(t)z^{g_{i1}^{ESc}} + p_2^{ESc}(t)z^{g_{i2}^{ESc}} = p_1^{ESc}(t)z^{540} + p_2^{ESc}(t)z^0.$

Converter: $L_z\{g^C(t)\} = p_1^C(t)z^{g_1^C} + p_2^C(t)z^{g_2^C} = p_1^C(t)z^{540} + p_2^C(t)z^0.$

Speed Reducer: $L_z\{g^{SR}(t)\} = p_1^{SR}(t)z^{g_1^{SR}} + p_2^{SR}(t)z^{g_2^{SR}} = p_1^{SR}(t)z^{540} + p_2^{SR}(t)z^0.$

Control Unit: $L_z\{g^{CU}(t)\} = p_1^{CU}(t)z^{g_1^{CU}} + p_2^{CU}(t)z^{g_2^{CU}} = p_1^{CU}(t)z^{540} + p_2^{CU}(t)z^0.$

4.2.2 Element with 3 States

The system's element, Energy Storage Serial (ESs), has 3 states: fully working state with performance 540 KW, partial failure state with performances 440 and fully failure. The state-space diagram is presented on Fig. 5. To calculate probabilities of each state we build the following system of differential equations:

$$\begin{cases} \frac{dp_1^{ESs}(t)}{dt} = -\lambda_{12}^{ESs}p_1^{ESs}(t) + \mu_{21}^{ESs}p_2^{ESs}(t) + \mu_{31}^{ESs}p_3^{ESs}(t), \\ \frac{dp_2^{ESs}(t)}{dt} = \lambda_{12}^{ESs}p_1^{ESs}(t) - (\lambda_{23}^{ESs} + \mu_{21}^{ESs})p_2^{ESs}(t) \\ \frac{dp_3^{ESs}(t)}{dt} = \lambda_{23}^{ESs}p_2^{ESs}(t) - \mu_{31}^{ESs}p_3^{ESs}(t) \end{cases}$$

Initial conditions are

$$p_1^{ESs}(0) = 1;\ p_2^{ESs}(0) = 0;\ p_3^{ESs}(0) = 0.$$

We used MATLAB® for numerical solution of this system of DE to obtain probabilities $p_1^{ESs}(t)$, $p_2^{ESs}(t)$, $p_3^{ESs}(t)$. Therefore, for such system's element the output performance stochastic processes can be obtained as follows:

$$\begin{cases} \mathbf{g}^{ESs} = \{g_1^{ESs}, g_2^{ESs}, g_3^{ESs}\} = \{540, 440, 0\}, \\ \mathbf{p}^{ESs}(t) = \{p_1^{ESs}(t), p_2^{ESs}(t), p_3^{ESs}(t)\}. \end{cases}$$

Sets $\mathbf{g}^{ESs}, \mathbf{p}^{ESs}(t)$ define *Lz*-transforms for Energy Storage Serial as follows:

$$L_z\{g^{ESs}(t)\} = p_1^{ESs}(t)z^{g_1^{ESs}} + p_2^{ESs}(t)z^{g_2^{ESs}} + p_{32}^{ESs}(t)z^{g_3^{ESs}} = p_1^{ESs}(t)z^{540} + p_2^{ESs}(t)z^{440} + p_3^{ESs}(t)z^0.$$

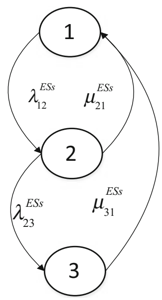

Fig. 5 Energy Storage Serial

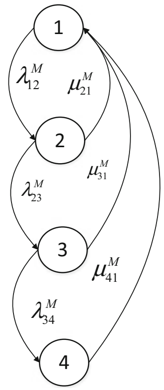

Fig. 6 State space diagram for Motor

4.2.3 Element with 4 States

The system's element, Motor (M), has 4 states: fully working state with performance 540 KW, two partial failure states with performances 480 and 420 KW and fully failure state. The state-space diagram is presented on Fig. 6. To calculate probabilities of each state we build the following system of differential equations:

$$\begin{cases} \frac{dp_1^M(t)}{dt} = -\lambda_{12}^M p_1^M(t) + \mu_{21}^M p_2^M(t) + \mu_{31}^M p_3^M(t) + \mu_{41}^M p_4^M(t), \\ \frac{dp_2^M(t)}{dt} = \lambda_{12}^M p_1^M(t) - (\lambda_{23}^M + \mu_{21}^M) p_2^M(t) \\ \frac{dp_3^M(t)}{dt} = \lambda_{23}^M p_2^M(t) - (\lambda_{34}^M + \mu_{31}^M) p_3^M(t) \\ \frac{dp_4^M(t)}{dt} = \lambda_{34}^M p_3^M(t) - \mu_{41}^M p_4^M(t) \end{cases}$$

Initial conditions are

$$p_1^M(0) = 1;\ p_2^M(0) = 0;\ p_3^M(0) = 0;\ p_4^M(0) = 0.$$

We used MATLAB® for numerical solution of this system of DE to obtain probabilities $p_1^M(t)$, $p_2^M(t)$, $p_3^M(t)$, $p_4^M(t)$. Therefore, for such system's element the output performance stochastic processes can be obtained as follows:

$$\begin{cases} \mathbf{g}^M = \{g_1^M, g_2^M, g_3^M, g_4^M\} = \{540, 480, 420, 0\}, \\ \mathbf{p}^M(t) = \{p_1^M(t), p_2^M(t), p_3^M(t), p_4^M(t)\}. \end{cases}$$

Sets $\mathbf{g}^M, \mathbf{p}^M(t)$ define Lz-transforms for each element as follows:

$$\begin{aligned} L_z\{g^M(t)\} &= p_1^M(t) z^{g_1^M} + p_2^M(t) z^{g_2^M} + p_3^M(t) z^{g_3^M} + p_4^M(t) z^{g_4^M} \\ &= p_1^M(t) z^{540} + p_2^M(t) z^{480} + p_3^M(t) z^{420} + p_4^M(t) z^{0}. \end{aligned}$$

4.3 Lz-Transform for Serial Topology System

4.3.1 Sub-System 1 (SS_{1s})

According to Fig. 2, Sub-system 1 consists of Fuel Tank, Gas Turbine and Generator, connected in series. Using the composition operator Ω_{fser}, we obtain the Lz-transform $L_z\{G^{SS_{1s}}(t)\}$ for the Sub-system 1, where the powers of z are found as minimum of powers of corresponding terms:

$$\begin{aligned} L_z\{G^{SS_{1s}}(t)\} &= \Omega_{f_{ser}}\left(L_z\{g^{FT}(t)\}, L_z\{g^{GT}(t)\}, L_z\{g^{G}(t)\}\right) \\ &= \Omega_{f_{ser}}\left(p_1^{FT}(t)z^{540} + p_2^{FT}(t)z^0, p_1^{GT}(t)z^{540} + p_2^{GT}(t)z^0, p_1^{G}(t)z^{540} + p_2^{G}(t)z^0\right) \\ &= p_1^{FT}(t)p_1^{GT}(t)p_1^{G}(t)z^{540} + \left(1 - p_1^{FT}(t)p_1^{GT}(t)p_1^{G}(t)\right)z^0. \end{aligned}$$

Using the following notations

$$\begin{aligned} P_1^{SS_{1s}}(t) &= p_1^{FT}(t)p_1^{GT}(t)p_1^{G}(t); \\ P_2^{SS_{1s}}(t) &= 1 - p_1^{FT}(t)p_1^{GT}(t)p_1^{G}(t); \end{aligned}$$

we obtain the resulting Lz-transform for the Sub-system 1 in the following form

$$L_z\{G^{SS_{1s}}(t)\} = P_1^{SS_{1s}}(t)z^{540} + P_2^{SS_{1s}}(t)z^0. \tag{5}$$

4.3.2 Sub-System 2 (SS_{2s})

Sub-system 2 consists of Converter, Motor and Control Unit, connected in series. Using the composition operator Ω_{fser}, where powers of z are calculated as minimum values of powers of corresponding terms, as before we obtain the Lz-transform $L_z\{G^{SS_{2s}}(t)\}$ for Sub-system 2 as follows:

$$\begin{aligned} L_z\{G^{SS_{2s}}(t)\} &= \Omega_{f_{ser}}\left(L_z\{g^{C}(t)\}, L_z\{g^{M}(t)\}, L_z\{g^{CU}(t)\}\right) \\ &= \Omega_{f_{par}}\left(p_1^{C}(t)z^{540} + p_2^{C}(t)z^0, p_1^{M}(t)z^{540} + p_2^{M}(t)z^{480} + p_3^{M}(t)z^{420} + p_4^{M}(t)z^0,\right. \\ &\quad \left. p_1^{CU}(t)z^{540} + p_2^{CU}(t)z^0\right). \end{aligned}$$

Using notations

$$\begin{aligned} P_1^{SS_{2s}}(t) &= p_1^{C}(t)p_1^{M}(t)p_1^{CU}(t); \\ P_2^{SS_{2s}}(t) &= p_1^{C}(t)p_2^{M}(t)p_1^{CU}(t); \\ P_3^{SS_{2s}}(t) &= p_1^{C}(t)p_3^{M}(t)p_1^{CU}(t); \\ P_4^{SS_{2s}}(t) &= p_1^{C}(t)p_4^{M}(t)p_1^{CU}(t) + p_1^{C}(t)p_2^{CU}(t) + p_2^{C}(t); \end{aligned}$$

we obtain the resulting *Lz*-transform for the Sub-system 2 in the following form

$$L_z\{G^{SS_{2s}}(t)\} = P_1^{SS_{2s}}(t)z^{540} + P_2^{SS_{2s}}(t)z^{480} + P_3^{SS_{2s}}(t)z^{420} + P_4^{SS_{2s}}(t)z^0.$$

4.3.3 Serial Topology System (STS)

Serial Topology System consists of Sub-system 1 and Sub-system 2, connected in series. Using the composition operator $\Omega_{f_{ser}}$, where powers of z are calculated as minimum values of powers of corresponding terms, in the same way as before we obtain the *Lz*-transform $L_z\{G^{STS}(t)\}$ for Serial Topology System as follows:

$$\begin{aligned} L_z\{G^{STS}(t)\} &= \Omega_{f_{ser}}\left(L_z\{G^{SS_{1s}}(t)\}, L_z\{G^{SS_{2s}}(t)\}\right) \\ &= \Omega_{f_{ser}}\left(P_1^{SS_{1s}}(t)z^{540} + P_2^{SS_{1s}}(t)z^0,\right. \\ &\quad \left. P_1^{SS_{2s}}(t)z^{540} + P_2^{SS_{2s}}(t)z^{480} + P_3^{SS_{2s}}(t)z^{420} + P_4^{SS_{2s}}(t)z^0\right) \end{aligned}$$

Using notations

$$\begin{aligned} P_1^{STS}(t) &= P_1^{SS_{1s}}(t)P_1^{SS_{2s}}(t); \\ P_2^{STS}(t) &= P_1^{SS_{1s}}(t)P_2^{SS_{2s}}(t); \\ P_3^{STS}(t) &= P_1^{SS_{1s}}(t)P_3^{SS_{2s}}(t); \\ P_4^{STS}(t) &= P_1^{SS_{1s}}(t)P_4^{SS_{2s}}(t) + P_2^{SS_{1s}}(t); \end{aligned}$$

we obtain the resulting *Lz*-transform for the Serial Topology System in the following form

$$L_z\{G^{STS}(t)\} = P_1^{STS}(t)z^{540} + P_2^{STS}(t)z^{480} + P_3^{STS}(t)z^{420} + P_4^{STS}(t)z^0. \quad (6)$$

4.3.4 Serial Topology System with Energy Storage (STS-ESs)

Serial Topology System with Energy Storage consists of Energy Storage and Sub-system 2, connected in series. Using the composition operator $\Omega_{f_{ser}}$, where powers of z are calculated as minimum values of powers of corresponding terms, as in previous instances we obtain the *Lz*-transform $L_z\{G^{STS-ESs}(t)\}$ for Serial Topology System with Energy Storage as follows:

$$
\begin{aligned}
L_z\{G^{STS-ESs}(t)\} &= \Omega_{f_{ser}}\left(L_z\{g^{ESs}(t)\}, L_z\{G^{SS_{1s}}(t)\}\right) \\
&= \Omega_{f_{par}}\left(p_1^{ESs}(t)z^{540} + p_2^{ESs}(t)z^{440} + p_3^{ESs}(t)z^0,\right. \\
&\quad \left. P_1^{SS_{1s}}(t)z^{540} + P_2^{SS_{1s}}(t)z^{480} + P_3^{SS_{1s}}(t)z^{420} + P_4^{SS_{1s}}(t)z^0\right).
\end{aligned}
$$

Using notations

$$
\begin{aligned}
&P_1^{STS-ESs}(t) = p_1^{ESs}(t)P_1^{SS_{1s}}(t); \\
&P_2^{STS-ESs}(t) = p_1^{ESs}(t)P_2^{SS_{1s}}(t); \\
&P_3^{STS-ESs}(t) = p_2^{ESs}(t)\left(P_1^{SS_{1s}}(t) + P_2^{SS_{1s}}(t)\right); \\
&P_4^{STS-ESs}(t) = \left(p_1^{ESs}(t) + p_2^{ESs}(t)\right)P_3^{SS_{1s}}(t); \\
&P_5^{STS-ESs}(t) = \left(p_1^{ESs}(t) + p_2^{ESs}(t)\right)P_4^{SS_{1s}}(t) + P_3^{SS_{1s}}(t);
\end{aligned}
$$

we obtain the resulting *Lz*-transform for the Serial Topology System with Energy Storage in the following form

$$
\begin{aligned}
L_z\{G^{STS-ESs}(t)\} &= P_1^{STS-ESs}(t)z^{540} + P_2^{STS-ESs}(t)z^{480} \\
&\quad + P_3^{STS-ESs}(t)z^{440} + P_4^{STS-ESs}(t)z^{420} + P_5^{STS-ESs}(t)z^0.
\end{aligned}
\tag{7}
$$

4.4 Lz-Transform for Combined Topology System

4.4.1 Sub-System 1 (SS_{1c})

Following Fig. 3. Sub-system 1 consists of Fuel Tank and Gas Turbine, connected in series. Using the composition operator $\Omega_{f_{ser}}$, we obtain the *Lz*-transform $L_z\{G^{SS_{1c}}(t)\}$ for the Sub-system 1, where the powers of z are found as minimum of powers of corresponding terms:

$$
\begin{aligned}
L_z\{G^{SS_{1c}}(t)\} &= \Omega_{f_{ser}}\left(L_z\{g^{FT}(t)\}, L_z\{g^{GT}(t)\}\right) \\
&= \Omega_{f_{ser}}\left(p_1^{FT}(t)z^{540} + p_2^{FT}(t)z^0, p_1^{GT}(t)z^{540} + p_2^{GT}(t)z^0\right) \\
&= p_1^{FT}(t)p_1^{GT}(t)z^{540} + \left(p_2^{FT}(t)p_1^{GT}(t) + p_2^{GT}(t)\right)z^0.
\end{aligned}
$$

Using the following notations

$$
\begin{aligned}
&P_1^{SS_{1c}}(t) = p_1^{FT}(t)p_1^{GT}(t); \\
&P_2^{SS_{1c}}(t) = p_2^{FT}(t)p_1^{GT}(t) + p_2^{GT}(t);
\end{aligned}
$$

we obtain the resulting *Lz*-transform for the Sub-system 1 in the following form

$$L_z\{G^{SS_{1c}}(t)\} = P_1^{SS_{1c}}(t)z^{540} + P_2^{SS_{1c}}(t)z^0.$$

4.4.2 Sub-System 2 (SS_2)

Sub-system 2 consists of Generator, Converter and Motor, connected in series. Using the composition operator Ω_{fser}, where powers of z are calculated as minimum values of powers of corresponding terms, as before we obtain the *Lz*-transform $L_z\{G^{SS_{2c}}(t)\}$ for Sub-system 2 as follows:

$$\begin{aligned} L_z\{G^{SS_{2c}}(t)\} &= \Omega_{f_{ser}}\left(L_z\{G^G(t)\}, L_z\{g^C(t)\}, L_z\{g^M(t)\}\right) \\ &= \Omega_{f_{ser}}\left(p_1^G(t)z^{540} + p_2^G(t)z^0, p_1^C(t)z^{540} + p_2^C(t)z^0, \right. \\ &\quad \left. p_1^M(t)z^{540} + p_2^M(t)z^{480} + p_3^M(t)z^{420} + p_4^M(t)z^0\right) \end{aligned}$$

Using notations

$$\begin{aligned} P_1^{SS_{2c}}(t) &= p_1^G(t)p_1^C(t)p_1^M(t); \\ P_2^{SS_{2c}}(t) &= p_1^G(t)p_1^C(t)p_2^M(t); \\ P_3^{SS_{2c}}(t) &= p_1^G(t)p_1^C(t)p_3^M(t); \\ P_4^{SS_{2c}}(t) &= p_1^G(t)p_1^C(t)p_4^M(t) + p_1^G(t)p_2^C(t) + p_2^G(t); \end{aligned}$$

we obtain the resulting *Lz*-transform for the Sub-system 2 in the following form

$$L_z\{G^{SS_{2c}}(t)\} = P_1^{SS_{2c}}(t)z^{540} + P_2^{SS_{2c}}(t)z^{480} + P_3^{SS_{2c}}(t)z^{420} + P_4^{SS_{2c}}(t)z^0.$$

4.4.3 Sub-System 3 (SS_3)

Sub-system 3 consists of Sub-system 2 and Speed Reducer, connected in parallel, where Speed Reducer is used as backup element. Using the composition operator Ω_{fpar}, where powers of z are calculated as maximum values of powers of corresponding terms, in the same way as before we obtain the *Lz*-transform $L_z\{G^{SS_{3c}}(t)\}$ for Sub-system 3 as follows:

$$\begin{aligned} L_z\{G^{SS_{3c}}(t)\} &= \Omega_{f_{ser}}\left(L_z\{G^{SS_{2c}}(t)\}, L_z\{g^{SR}(t)\}\right) \\ &= \Omega_{f_{par}}\left(P_1^{SS_{2c}}(t)z^{540} + P_2^{SS_{2c}}(t)z^{480} + P_3^{SS_{2c}}(t)z^{420} + P_4^{SS_{2c}}(t)z^0, \right. \\ &\quad \left. p_1^{SR}(t)z^{540} + p_2^{SR}(t)z^0\right). \end{aligned}$$

Using notations

$$P_1^{SS_{3c}}(t) = p_1^{SR}(t) + P_1^{SS_{2c}}(t)p_2^{SR}(t);$$
$$P_2^{SS_{3c}}(t) = P_2^{SS_{2c}}(t)p_2^{SR}(t);$$
$$P_3^{SS_{3c}}(t) = P_3^{SS_{2c}}(t)p_2^{SR}(t);$$
$$P_4^{SS_{3c}}(t) = P_4^{SS_{2c}}(t)p_2^{SR}(t);$$

we obtain the resulting *Lz*-transform for the Sub-system 3 in the following form

$$L_z\{G^{SS_{3c}}(t)\} = P_1^{SS_{3c}}(t)z^{540} + P_2^{SS_{3c}}(t)z^{480} + P_3^{SS_{3c}}(t)z^{420} + P_4^{SS_{3c}}(t)z^0.$$

4.4.4 Combined Topology System (CTS)

Combined Topology System consists of Sub-System 1, Subsystem 3 and Control Unit, connected in series. Using the composition operator Ω_{fser}, where powers of z are calculated as minimum values of powers of corresponding terms, as in previous instances we obtain the *Lz*-transform $L_z\{G^{CTS}(t)\}$ for Combined Topology System as follows:

$$\begin{aligned} L_z\{G^{CTS}(t)\} &= \Omega_{f_{ser}}\left(L_z\{G^{SS_1}(t)\}, L_z\{G^{SS_{3c}}(t)\}, L_z\{g^{CU}(t)\}\right) \\ &= \Omega_{f_{ser}}\left(P_1^{SS_{1c}}(t)z^{540} + P_2^{SS_{1c}}(t)z^0,\right. \\ &\quad \left. P_1^{SS_{3c}}(t)z^{540} + P_2^{SS_{3c}}(t)z^{480} + P_3^{SS_{3c}}(t)z^{420} + P_4^{SS_{3c}}(t)z^0, p_1^{CU}(t)z^{540} + p_2^{CU}(t)z^0\right). \end{aligned}$$

Using notations

$$P_1^{CTS}(t) = P_1^{SS_{1c}}(t)P_1^{SS_{3c}}(t)p_1^{CU}(t);$$
$$P_2^{CTS}(t) = P_1^{SS_{1c}}(t)P_2^{SS_{3c}}(t)p_1^{CU}(t);$$
$$P_3^{CTS}(t) = P_1^{SS_{1c}}(t)P_3^{SS_{3c}}(t)p_1^{CU}(t);$$
$$P_4^{CTS}(t) = P_1^{SS_{1c}}(t)\left(1 - P_4^{SS_{3c}}(t)\right)p_2^{CU}(t) + P_1^{SS_{1c}}(t)P_4^{SS_{3c}}(t) + P_2^{SS_{1c}}(t);$$

we obtain the resulting *Lz*-transform for the Combined Topology System in the following form

$$L_z\{G^{CTS}(t)\} = P_1^{CTS}(t)z^{540} + P_2^{CTS}(t)z^{480} + P_3^{CTS}(t)z^{420} + P_4^{CTS}(t)z^0. \quad (8)$$

4.4.5 Combined Topology System with Energy Storage (CTS-ESc)

Combined Topology System with Energy Storage consists of Combined Energy Storage, Converter, Motor and Control Unit, connected in series. Using the composition operator Ω_{fser}, where powers of z are calculated as minimum values of powers of corresponding terms, in the same way as before, we obtain the Lz-transform $L_z\{G^{CTS-ESc}(t)\}$ for Combined Topology System with Energy Storage as follows:

$$\begin{aligned} L_z\{G^{CTS-ESc}(t)\} &= \Omega_{f_{ser}}\left(L_z\{g^{ESc}(t)\}, L_z\{g^{C}(t)\}, L_z\{g^{M}(t)\}, L_z\{g^{CU}(t)\}\right) \\ &= \Omega_{f_{par}}\left(p_1^{ESc}(t)z^{540} + p_2^{ESc}(t)z^{0}, p_1^{C}(t)z^{540} + p_2^{C}(t)z^{0},\right. \\ &\quad \left. p_1^{M}(t)z^{540} + p_2^{M}(t)z^{480} + p_3^{M}(t)z^{420} + p_4^{M}(t)z^{0},\ p_1^{CU}(t)z^{540} + p_2^{CU}(t)z^{0}\right) \end{aligned}$$

Using simple algebra calculations of the powers of z as minimum values of powers of corresponding terms and the following notations

$$\begin{aligned} P_1^{CTS-ESc}(t) &= p_1^{ESc}(t)p_1^{C}(t)p_1^{M}(t)p_1^{CU}(t); \\ P_2^{CTS-ESc}(t) &= p_1^{ESc}(t)p_1^{C}(t)p_2^{M}(t)p_1^{CU}(t); \\ P_3^{CTS-ESc}(t) &= p_1^{ESc}(t)p_1^{C}(t)p_3^{M}(t)p_1^{CU}(t); \\ P_4^{CTS-ESc}(t) &= p_1^{ESc}(t)p_1^{C}(t)\left(p_2^{CU}(t) + p_4^{M}(t)p_1^{CU}(t)\right) + p_1^{ESc}(t)p_2^{C}(t) + p_2^{ESc}(t); \end{aligned}$$

the whole system's Lz-transform expression is as follows:

$$\begin{aligned} L_z\{G^{CTS-ESc}(t)\} = P_1^{CTS-ESc}(t)z^{540} + P_2^{CTS-ESc}(t)z^{480} \\ + P_3^{CTS-ESc}(t)z^{420} + P_4^{CTS-ESc}(t)z^{0}. \end{aligned} \quad (9)$$

5 Availability and Mean Power Performance Calculation

Using expression (3), the MSS mean instantaneous availability for constant demand level w may be presented as follows:

- For w = 540 KW demand level

$$\begin{aligned} A_{w=540KW}^{STS}(t) &= \sum_{g_k \geq 540} P_k^{STS}(t) = P_1^{STS}(t) \\ A_{w=540KW}^{CTS}(t) &= \sum_{g_k \geq 540} P_k^{CTS}(t) = P_1^{CTS}(t) \end{aligned} \quad (10)$$

- For w = 460 KW demand level

$$\begin{aligned} A_{w=460KW}^{STS}(t) &= \sum_{g_k \geq 460} P_k^{STS}(t) = P_1^{STS}(t) + P_2^{STS}(t) \\ A_{w=460KW}^{CTS}(t) &= \sum_{g_k \geq 460} P_k^{CTS}(t) = P_1^{CTS}(t) + P_2^{CTS}(t) \end{aligned} \quad (11)$$

- For w = 360 KW demand level

$$\begin{aligned} A^{STS}_{w=360KW}(t) &= \sum_{g_k \geq 360} P^{STS}_{k}(t) = \sum_{i=1}^{4} P^{STS}_{i}(t) \\ A^{CTS}_{w=360KW}(t) &= \sum_{g_k \geq 360} P^{CTS}_{k}(t) = \sum_{i=1}^{3} P^{CTS}_{i}(t) \end{aligned} \tag{12}$$

Using expression (4), the MSS instantaneous mean power performance for the Serial and Combined Topology Systems can be obtained as follows:

$$\begin{aligned} E^{STS}(t) &= \sum_{g_s > 0} g_i^{STS} P_i^{STS}(t) = \sum_{i=1}^{4} g_i^{STS} P_i^{STS}(t) \\ &= 540P_1^{STS}(t) + 480P_2^{STS}(t) + 440P_3^{STS}(t) + 420P_4^{STS}(t) \\ E^{CTS}(t) &= \sum_{g_s > 0} g_i^{CTS} P_i^{CTS}(t) = \sum_{i=1}^{3} g_i^{CTS} P_i^{CTS}(t) \\ &= 540P_1^{CTS}(t) + 480P_2^{CTS}(t) + 420P_3^{CTS}(t) \end{aligned} \tag{13}$$

The failure and repair rates (in year^{-1}) of each system's elements are presented in the Table 1.

MSS mean instantaneous availability for different constant demand levels is presented in Figs. 7 and 8. The obtained results shows that difference in instantaneous availability for Serial Topology System for different demand levels is small enough (Fig. 7), for Combined Topology System there is no distinction for different demand levels (Fig. 8).

Comparison MSS mean instantaneous availability levels for different topology shows that Combined Topology is better than Serial Topology (Figs. 9 and 10). In case of emergency and usage of Energy Storage the instantaneous availability of Serial system is greater than Combined Topology System (Fig. 11).

Table 1 Failure and repair rates of each system's elements

	Failure rates (year^{-1})	Repair rates (year^{-1})
Fuel tank (FT)	0.0584	219
Gas turbine (GT)	0.876	159
Generator (G)	0.0145	175.2
Energy Storage Series (ESs)	0.438	438
Energy Storage Combined (ESc)	0.438	250
Electric inverter (C)	0.0584	584
Motor (M)	0.0145	87.6
Speed reducer (SR)	0.0876	116.8
Control unit (CU)	0.01752	730

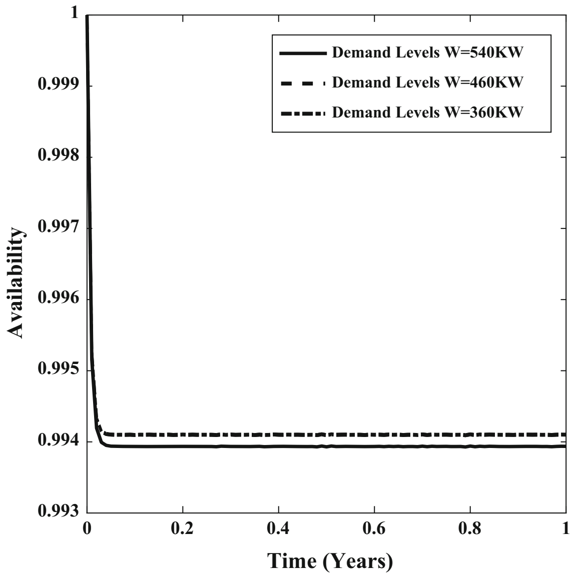

Fig. 7 MSS mean instantaneous availability for Serial Topology System for different demand levels

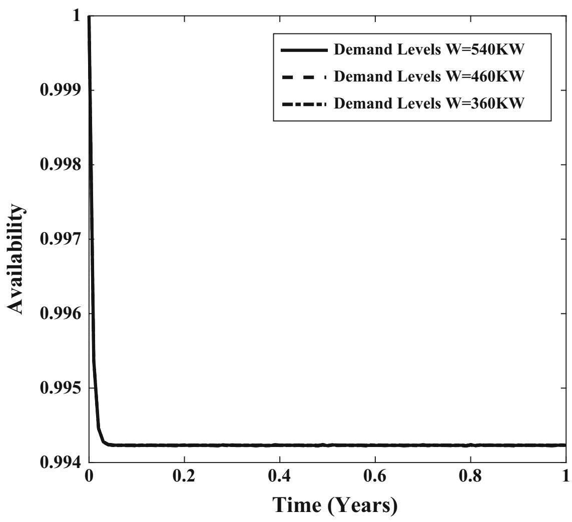

Fig. 8 MSS mean instantaneous availability for Combined Topology System for different demand levels

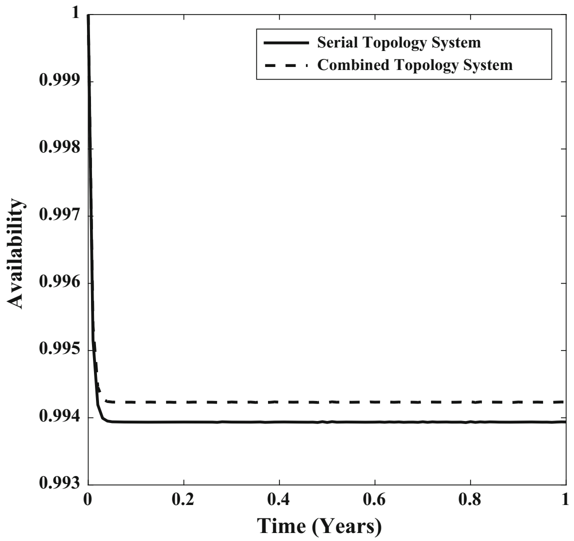

Fig. 9 MSS mean instantaneous availability for Serial and Combined Topology System for w = 540 KW

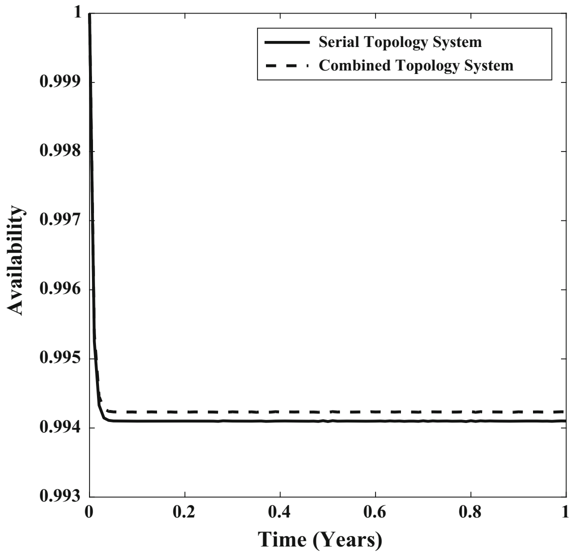

Fig. 10 MSS mean instantaneous availability for Serial and Combined Topology System for w = 460 KW

Fig. 11 MSS mean instantaneous availability for Serial and Combined Topology System with energy storage

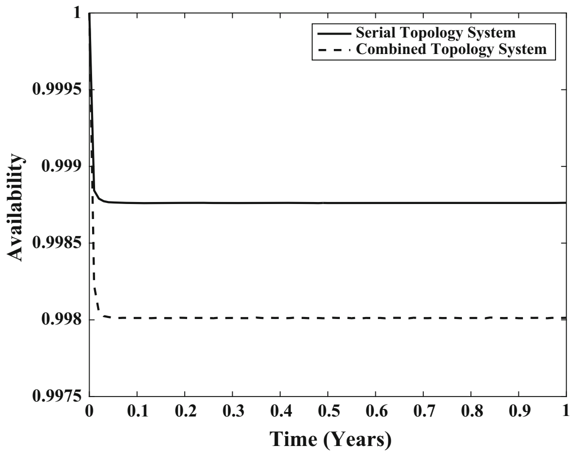

Fig. 12 MSS instantaneous mean power performance of the Serial and Combined Topology Systems

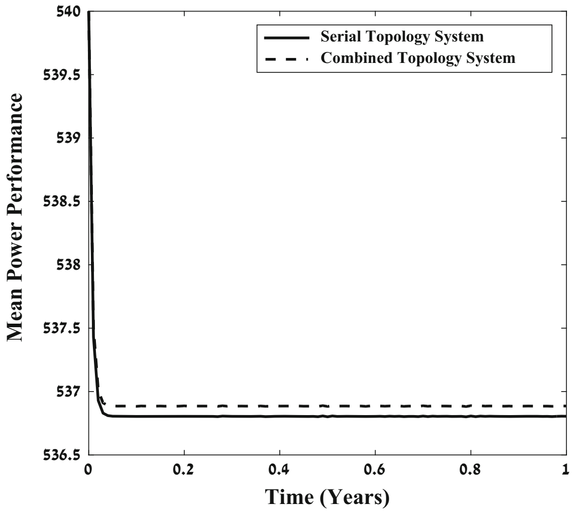

Calculated MSS instantaneous mean power performance of the Serial and Combined Topology System is presented in Fig. 12.

6 Conclusion

In this chapter, the *Lz*-transform method was used for evaluation of two important parameters—availability and performance of various topologies traction drives of hybrid-electric helicopter.

Lz-transform approach extremely simplifies the solution, which in comparison with straightforward Markov method would have required building and solving the model with 128 states for Serial and 512 states for Combined Topology Systems.

The obtained results have showed that in terms of reliability the compared variants of traction drive topologies of hybrid-electric helicopter are close enough and meet the requirements of the project. Considering this, to select the optimal variant, it is necessary to carry out a comparative analysis of their weight and size characteristics.

Nine-phase design of the traction permanent magnets synchronous motor is the best compromise solution between the required level of its fault tolerance and the complexity of manufacturing.

References

1. Bolvashenkov I, Herzog H-G (2016) Use of stochastic models for operational efficiency analysis of multi power source traction drives. In: Frenkel I, Lisnianski A (eds) Proceedings of the second international symposium on stochastic models in reliability engineering, life science and operations management, SMRLO'16, Beer Sheva, Israel, 15–18 Feb 2016. IEEE CPS, pp 124–130. doi:10.1109/SMRLO.2016.30
2. Bolvashenkov I, Frenkel I, Kammermann J, Herzog H-G (2017) The choice of an optimal structure and parameters of energy storage for an electrical helicopter traction drive. In: Proceedings of IEEE twelfth international conference on ecological vehicles and renewable energies (EVER'17), 11–13 Apr 2017, Monaco, pp 1–6
3. Bolvashenkov I, Kammermann J, Lahlou T, Herzog H-G (2016) Comparison and choice of a fault tolerant inverter topology for the traction drive of an electrical helicopter. In: 3rd international conference on electrical systems for aircraft, railway, ship propulsion, and road vehicles (ESARS'16), 02–04 Nov 2016, Toulouse, France, pp 1–6
4. Bolvashenkov I, Kammermann J, Willerich S, Herzog H-G (2016) Comparative study of reliability and fault tolerance of multi-phase permanent magnet synchronous motors for safety-critical drive trains. In: Proceedings of international conference on renewable energies and power quality (ICREPQ'16), 4–6 May Madrid, Spain, pp 1–6
5. Frenkel I, Bolvashenkov I, Herzog H-G, Khvatskin L (2016) Performance availability assessment of combined multi power source traction drive considering real operational conditions. Transp Telecommun 17(3):179–191. doi:10.1515/ttj-2016-0016
6. Frenkel I, Bolvashenkov I, Herzog H-G, Khvatskin L (2017) Operational sustainability assessment of multipower source traction drive. In: Mathematics applied to engineering. Elsevier Ltd. pp 191–203. doi:10.1016/B978-0-12-810998-4.00010-7
7. Huang H (2015) Challenges in more electric aircraft (MEA). IEEE Transp Electr Newslett, July/August, 2015
8. Jia H, Jin W, Ding Y, Song Y, Yu D (2017) Multi-state time-varying reliability evaluation of smart grid with flexible demand resources utilizing *Lz*-transform. In: Proceeding of the international conference on energy engineering and environmental protection (EEEP2016), IOP Publishing, IOP conference series: Earth and Environmental Science, vol 52, p 012011. doi:10.1088/1755-1315/52/1/012011
9. Lahne HC, Staton D, Chong YC, Gerling D (2016) Design of a 50000 rpm high-speed high-power six-phase PMSM for use in aircraft applications. In: Proceedings of IEEE eleventh international conference on ecological vehicles and renewable energies (EVER'16), 06–08 Apr 2016, Monaco, pp 1–11

10. Lisnianski A (2012) *LZ*-transform for a discrete-state continuous-time markov process and its application to multi-state system reliability. In: Lisnianski A, Frenkel I (eds) Recent advances in system reliability. Signatures, multi-state systems and statistical inference. Springer, London, pp 79–95
11. Lisnianski A, Ben Haim H (2013) Short-term reliability evaluation for power stations by using Lz-transform. J Mod Power Syst Clean Energy 1(2):110–117. doi:10.1007/s40565-013-0021-3
12. Lisnianski A, Frenkel I, Ding Y (2010) Multi-state system reliability analysis and optimization for engineers and industrial managers. Springer, London
13. Natvig B (2011) Multistate systems reliability. Theory with applications. Wiley, New York
14. Rieger H. Hubschraubertyp Airbus Helicopters EC 135. http://www.rth.info/typen/typen.php?show=ec135
15. Rick H (2013) Gasturbinen und Flugantriebe: Grundlagen, Betriebsverhalten and Simulation. Springer, Berlin
16. Sheu S-H, Zang ZC (2013) An optimal age replacement policy for multi-state systems. IEEE Trans Reliab 62(3):722–733
17. Trivedi K (2002) Probability and statistics with reliability, queuing and computer science applications. Wiley, New York
18. Ushakov I (1986) A universal generating function. Sov J Comput Syst Sci 24:37–49